XL CILAMCE
IBERO-LATIN AMERICAN CONGRESS ON COMPUTATIONAL METHODS IN ENGINEERING
NOVEMBER 11-14, 2019
Praiamar Natal Hotel & Convention Natal, RN-BRAZIL

NUMERICAL SIMULATION AND EXPERIMENTAL ANALYSIS FOR THE BUBBLE GROWTH RADIUS BY CONSIDERING THE FLUID-SURFACE INTERACTION

Mateus Faria de Andrade Paschoal
Leonardo Lachi Manetti
João Batista Campos Silva
Elaine Maria Cardoso
mateus.f.a.p@gmail.com
leonardo.manetti@unesp.br
campos.silva@unesp.br
elaine.cardoso@unesp.br
UNESP/São Paulo State University, Post-Graduation Program in Mechanical Engineering, Av. Brasil, 56, 15385-000, Ilha Solteira, SP, Brazil

Abstract. *The advance of new technologies, associated with the minimization of manufacturing and installation costs, presents a great challenge for the refrigeration area since the heat generation has increased in recent years. Several studies have shown the influence of surface topography on the heat transfer performance, a strategic subject for the development of techniques for cooling of miniaturized electronic components, thermal control of satellites, cooling of high concentration photovoltaic cells and others. The objective of this work is to develop a theoretical and numerical study of the heat transfer phenomenon with phase change involving pool boiling, taking into account the influence of the heating surface characteristics and the use of different fluids (e.g., water or refrigerants) by the numerical simulation of a vapor bubble dynamic onto the heating surface. A computational code is developed in Fortran 90 language to solve the continuity, momentum, energy and interface capture equations in three-dimensional spherical coordinates. Moreover, it is implemented a method to capture the interface based on the coupled algorithm of Volume of Fluid Method and Level Set Method (CVOFLS). The effects of microlayer, contact angle and surface tension on the vapor bubble dynamic are also considered. The CVOFLS algorithm also allows the simulation in Eulerian fixed mesh. The finite element method is applied for space discretization and the Characteristic Based Split scheme (CBS) is applied for time discretization. The comparison with experimental data obtained by the research group and by other researchers is used to validate the numerical model. Thus, the rate of bubble growth and the bubble shape could be predicted until its departure time taking into account the effects of microlayer and surface/fluid interaction.*

Keywords: Pool Boiling, fem-CBS, CVOFLS

1 Introduction

The boiling process has large applicability in industries nowadays such as in the electronic devices. The boiling allows high heat fluxes exchange with a small temperature difference between the fluid and the heated surface (Yeom, Sridharan e Corradini [1]). In order to apply the boiling to increase the heat transfer performance of a thermal system, it is needed to fully understand the phenomenon. Some researchers studied the microlayer influence (Stephan and Hammer [2]; Kawanami et al. [3]), others the gravity acceleration (Wang et al. [4]) and some recent works analyzed the phenomenon with the addition of nanoparticles into the fluid refrigerant (Manetti et al. [5]).

Patil [6] presented two approaches to bubble dynamics – considering and not considering the microlayer in his formulation. In his approach, he considered a fixed mesh to external fluid around the bubble by adequately chose a non-dimensionalization of the variables in such a way that the bubble contour does not move. So, the governing equations were solved for a Eulerian mesh.

Shah and Talat [7] applied the moving mesh method to capture the interface. Although it is a very precise method to capture the interface, it demands too much computational cost. One other method used by these authors was the Characteristic Based Method (CBS). According to Baggio and Silva [8], this method is a very efficient split in the formulation allowing to use a simple discretization method like Galerkin finite element method with a stable solution.

Perez-Raya and Kandlikar [9], Teodori et al. [10] and Albadawi et al. [11], for example, deal with bubble moving mesh applying the Volume of Fluid Method (VOF). This method follows the liquid-vapor interface by the velocity field. The VOF is a method based on mass conservation; however, it is not a very precise method to interface tracking.

Another method for interface capturing is the Level Set Method (LS). This method has the advantage of estimate very accurately the interface. However, its formulation does not satisfy precisely the mass conservation, (Giboua et al. [12], Menon [13]).

In order to use the advantages of Volume of Fluid Method and Level Set Method some authors, for example, Ling et al. [14] and Albadawi et al. [15] mixed both methods into one: Coupled Volume of Fluid and Level Set Method (CVOFLS); with this method, it is possible to determine the interface precisely and the phase change layer with a static mesh.

For the mentioned works, the governing equations were written in Cartesian or cylindrical coordinates. However, according to Patil [6] and Pastuszko [16], the vapor bubble remains almost spherical during all time of its growth in pool boiling regime.

Based on that, this work presents a numerical simulation for a single bubble dynamics in three-dimensional spherical coordinates using the CBS and CVOFLS methods programmed in Fortran 90.

2 Basic Equations and Numerical Setup

In this topic will be presented the basic equations for fluid dynamics and for the methods used. Then, some numerical details are also presented.

2.1 Coupled Volume of Fluid and Level Set Method (CVOFLS)

According to Albadawi et al. [15], CVOFLS is solved in two steps:

- By solving the Advection Equation of Volume of Fluid Method;
- By correcting the interface by the Level Set Method.

In order to describe the method, first we need to introduce the Void Fraction α, that is defined in Eq. 1.

$$\begin{cases} \alpha=0, \text{ at gaseous phase} \\ 0<\alpha<1, \text{ at interface} \\ \alpha = 1, \text{ at liquid phase} \end{cases} \tag{1}$$

By considering a given multi-phase fluid system under a velocity field influence, the velocity field determines the transport of the void fraction according to Eq. (2):

$$\frac{\partial \alpha}{\partial t} + \nabla.\left(\alpha \vec{u}\right) = 0 \tag{2}$$

where $\vec{u}$ is the fluid velocity field.

As the void fraction is known, we can correct this variable by the Level Set Function by using the Eq. (3).

$$\frac{\partial \phi}{\partial \tau} + \text{sgn}\left(\phi_0\right)\left(\left|\nabla \phi\right| - 1\right) = 0 \tag{3}$$

where ϕ is the Level Set Function, defined in Eq. (4), ϕ_0 is an initial guess to ϕ, Eq. (5), and τ is a pseudo time step, defined as $\Delta\tau = 0.1\Delta x$. Δx is the smallest distance between two consecutive points in the generated mesh.

$$\phi = \begin{cases} \text{-1, at gaseous phase} \\ \text{0, at interface} \\ \text{1, at liquid phase} \end{cases} \tag{4}$$

$$\phi_0 = \left(2\alpha - 1\right)\Gamma \tag{5}$$

$$\Gamma = 0.25\Delta x \tag{6}$$

According to Albadawi et al. [15], Eq. (3) converges in φ_{cor} iterations. In addition, φ_{cor} is defined as:

$$\phi_{cor} = \frac{\varepsilon}{\Delta \tau} \tag{7}$$

$$\varepsilon = 1.5\Delta x \tag{8}$$

The advantage of this method is that both, α and ϕ, are functions that allow the domain to be formulated as monophasic. In order to predict the properties of each fluid, the following correlations are proposed:

$$\rho = \rho_g + \left(\rho_l - \rho_g\right)H \tag{9}$$

$$\mu = \mu_g + \left(\mu_l - \mu_g\right)H \tag{10}$$

where ρ is the fluid density, μ the dynamic viscosity and the subscripts l and g corresponding to liquid and gas phase. H is the Heaviside Function, described in Eq. (11):

$$H = \begin{cases} 0 & \text{se } \phi < -\varepsilon \\ \frac{1}{2}\left[1 + \frac{\phi}{\varepsilon} + \frac{1}{\pi}\sin\left(\frac{\pi\phi}{\varepsilon}\right)\right] & \text{se } |\phi| \leq -\varepsilon \\ 1 & \text{se } \phi > \varepsilon \end{cases} \tag{11}$$

2.2 Fluid dynamic equations

By using CLSVOF method, the mass, momentum and energy equations can be written as Eq. (12), Eq. (13) and Eq. (14).

$$\nabla \cdot \vec{u} = 0 \tag{12}$$

$$\rho\left(\frac{\partial \vec{u}}{\partial t} + \left(\vec{u} - \vec{u}^{c}\right) \cdot \nabla \vec{u}\right) = \rho \vec{g} \cos\chi - \nabla p + \mu \nabla^2 \vec{u} + \sigma \kappa \nabla H \tag{13}$$

$$\rho c_p \left(\frac{\partial T}{\partial t} + \left(\vec{u} - \vec{u}^{c}\right) \cdot \nabla T\right) = k \nabla^2 T + S \tag{14}$$

where $\vec{g}$ is the gravity acceleration vector, χ the angle between the horizontal surface and the heated surface, p is the pressure field, σ the superficial tension, c_p the heat capacity at constant pressure, T the temperature field, t the elapsed time, k the thermal conductivity and κ the interface curvature, written in Eq. (15) as:

$$\kappa = \nabla \cdot \vec{n}\,;\ \vec{n} = \frac{\nabla \phi}{|\nabla \phi|} \tag{15}$$

Equations (12), (13) and (14) were discretized by a Galerkin finite element method stabilized by the CBS scheme. Baggio and Silva [8] has more details about this method. After applying the CBS, the method used to discretize these equations was the Galerkin Finite Element Method. Equations (2) and (3) were discretized by Least Square Finite Element Method due to this equation be adjective dominant.

2.3 Numerical Details

In order to discretize the domain, presented in Fig. 1, it was used linear tetrahedral elements.

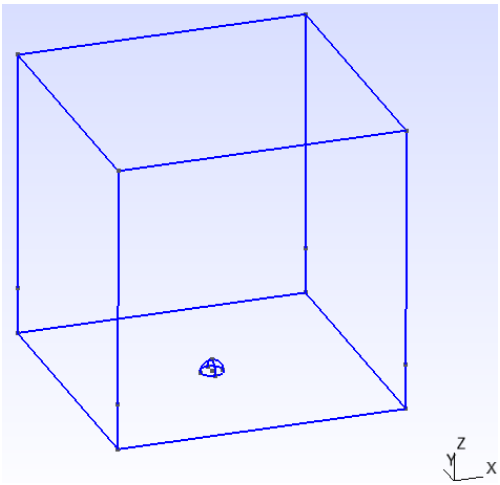

Figure 1. Computational Domain.

The time step was calculated based on Sato and Niceno [17], as described in Eq. (16).

$$\Delta t_{\min} = \min\left[C_{CFL} \frac{\Delta x}{|\vec{u}_{\max}|}; C_{st} \left(\frac{\rho_v \Delta x^3}{2\pi\sigma}\right)^{1/2} \right] \tag{16}$$

where $\vec{u}_{\max}$ is the maximum mesh velocity, $C_{CFL} = 0,25$, $C_{st} = \left(\frac{\overline{\rho} \Delta x^3}{2\pi\sigma} \right)^{1/2}$ and $\overline{\rho} = \frac{\rho_l + \rho_v}{2}$.

The numerical integration was done by Gauss Quadrature and the systems generated by fem-CBS were solved by Pre-Conditioned Gradient Method, as described by Press et al. [18].

The initial and boundary conditions of the problem are the following:

At $z=z_{inf}$

$$\begin{cases} u\left(x,y,z_{\inf},t\right) = v\left(x,y,z_{\inf},t\right) = w\left(x,y,z_{\inf},t\right) = 0 \\ T\left(x,y,z_{\inf},t\right) = T_s \\ P\left(x,y,z_{\inf},t\right) = P_{sat}\left(T_s\right) \\ \nabla\alpha.\overrightarrow{n_s} = \nabla\phi.\overrightarrow{n_s} = \cos\psi \end{cases}$$

At $z=z_{up}$

$$\begin{cases} u\left(x,y,z_{up},t\right) = v\left(x,y,z_{up},t\right) = w\left(x,y,z_{up},t\right) = 0 \\ T\left(x,y,z_{up},t\right) = T_\infty \\ P\left(x,y,z_{up},t\right) = P_{sat}\left(T_\infty\right) \\ \nabla\alpha = \nabla\phi = 0 \end{cases}$$

At $y=y_{left}$

$$\begin{cases} u\left(x,\mathrm{y}_{\text{left}},z,t\right) = v\left(x,\mathrm{y}_{\text{left}},z,t\right) = w\left(x,\mathrm{y}_{\text{left}},z,t\right) = 0 \\ T\left(x,\mathrm{y}_{\text{left}},z,t\right) = T_\infty \\ P\left(x,\mathrm{y}_{\text{left}},z,t\right) = P_{sat}\left(T_\infty\right) \\ \nabla\alpha = \nabla\phi = 0 \end{cases}$$

At $y=y_{right}$

$$\begin{cases} u\left(x,\mathrm{y}_{\text{right}},z,t\right) = v\left(x,\mathrm{y}_{\text{right}},z,t\right) = w\left(x,\mathrm{y}_{\text{right}},z,t\right) = 0 \\ T\left(x,\mathrm{y}_{\text{right}},z,t\right) = T_\infty \\ P\left(x,\mathrm{y}_{\text{right}},z,t\right) = P_{sat}\left(T_\infty\right) \\ \nabla\alpha = \nabla\phi = 0 \end{cases}$$

At $x=x_{front}$

$$\begin{cases} u\left(\mathrm{x}_{front},y,z,t\right) = v\left(\mathrm{x}_{front},y,z,t\right) = w\left(\mathrm{x}_{front},y,z,t\right) = 0 \\ T\left(\mathrm{x}_{front},y,z,t\right) = T_\infty \\ P\left(\mathrm{x}_{front},y,z,t\right) = P_{sat}\left(T_\infty\right) \\ \nabla\alpha = \nabla\phi = 0 \end{cases}$$

At $x=x_{back}$

$$\begin{cases} u(x_{back},y,z,t)=v(x_{back},y,z,t)=w(x_{back},y,z,t)=0 \\ T(x_{back},y,z,t)=T_{\infty} \\ P(x_{back},y,z,t)=P_{sat}(T_{\infty}) \\ \nabla\alpha=\nabla\phi=0 \end{cases}$$

Initial Condictions:

$$\begin{cases} u(x,y,z,0)=v(x,y,z,0)=w(x,y,z,0)=0 \\ \begin{cases} \text{To the fuid (liquid phase) outside the bubble} \\ T(x,y,z,0)=T_{\infty} \\ P(x,y,z,0)=P_{sat}(T_{\infty}) \\ \alpha=\phi=1 \end{cases} \\ \begin{cases} \text{To the fluid (gaseous phase) inside the bubble} \\ T(x,y,z,0)=T_{s} \\ P(x,y,z,0)=P_{sat}(T_{s}) \\ \alpha=0 \\ \phi=-1 \end{cases} \\ \begin{cases} \text{At surface } z=z_{inf} \\ T(x,y,z,0)=T_{s} \\ P(x,y,z,0)=P_{sat}(T_{s}) \end{cases} \\ \begin{cases} \text{To interface points} \\ \alpha=0.5 \\ \phi=0 \end{cases} \end{cases}$$

3 Experimental Setup

The tests were performed in the pool boiling apparatus (Fig. 2) that consists of a rectangular glass (120 × 100 mm²) with a thickness of 5 mm and 200 mm height. The upper and lower bases consisted of two stainless steel plates, 200 × 200 × 10 mm³. A thermal bath, Model Q214M2 operated with water, was used to control the condenser temperature located at the top of the boiling chamber. An auxiliary heater submerged in the working fluid was used to maintain the liquid temperature near the saturation point. Two K-type thermocouples, $T_{liq,}$ and T_{vap}, located in the working fluid and vapor, respectively, allowed monitoring the test condition temperature. The pressure inside the boiling chamber was measured by a pressure transducer and maintained at p_{atm} = 98 kPa (local atmospheric pressure) during the boiling tests. The pressure uncertainty is ± 0.05 kPa.

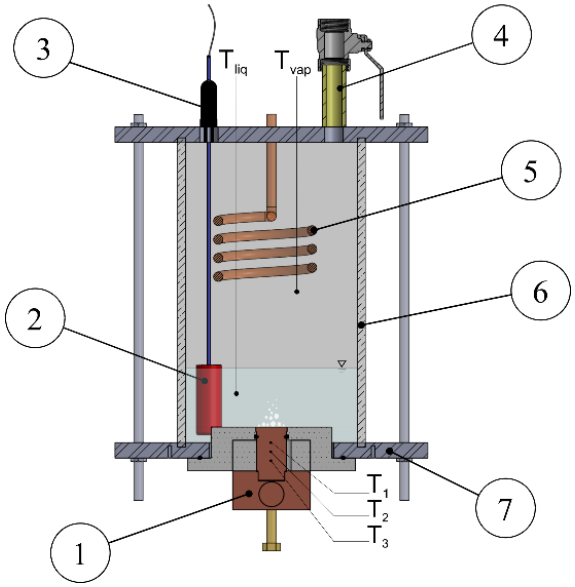

Figure 2. Pool boiling apparatus:(1) cooper block; (2) auxiliary heater; (3) Pressure transducer; (4) Vacuum/Feed Valve; (5) Condenser; (6) glass chamber; (7) Stainless steel plate.

The test section, Fig. 3, consisted of a copper piece with a square face at the top surface (16 × 16 × 3 mm^3) mounted on a copper block with 16 mm diameter. The copper block (60 mm height) had three K-type thermocouples with 0.5 mm diameters, which were used to estimate the wall temperature (T_w) and the heat flux ($q''_{measured}$). A cartridge resistance heated the copper block. The thermal insulation of the test section consisted of polytetrafluoroethylene.

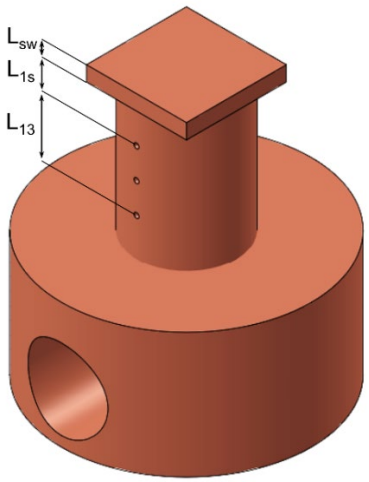

Figure 3. Test section view, including the position of the thermocouples.

Numerical simulation results were compared with experimental results for pool boiling of HFE7100, at saturation conditions and for low heat flux values (< 30 kW/m^2), on the plain copper surface described above.

4 Validation of CVOFLS Code

In order to validate the implemented code of Coupled Volume of Fluid and Level Set Method to determine the bubble interface, a benchmark problem described in Sato and Niceno [19] was used: a

vapor bubble radius of 0.15 units centered in (0.35, 0.35, 0.35) inside a cubic liquid domain with 1x1x1 units. Figure 4 shows the expected results.

$$u(x,y,z,t) = 2\cos\left(\frac{\pi t}{T}\right)\sin^2(\pi x)\sin(2\pi y)\sin(2\pi z) \tag{17}$$

$$v(x,y,z,t) = -\cos\left(\frac{\pi t}{T}\right)\sin(2\pi x)\sin^2(\pi y)\sin(2\pi z) \tag{18}$$

$$w(x,y,z,t) = -\cos\left(\frac{\pi t}{T}\right)\sin(2\pi x)\sin(2\pi y)\sin^2(\pi z) \tag{19}$$

where (x,y,z) corresponds to the mesh points coordinates and T is the period chosen by the user.

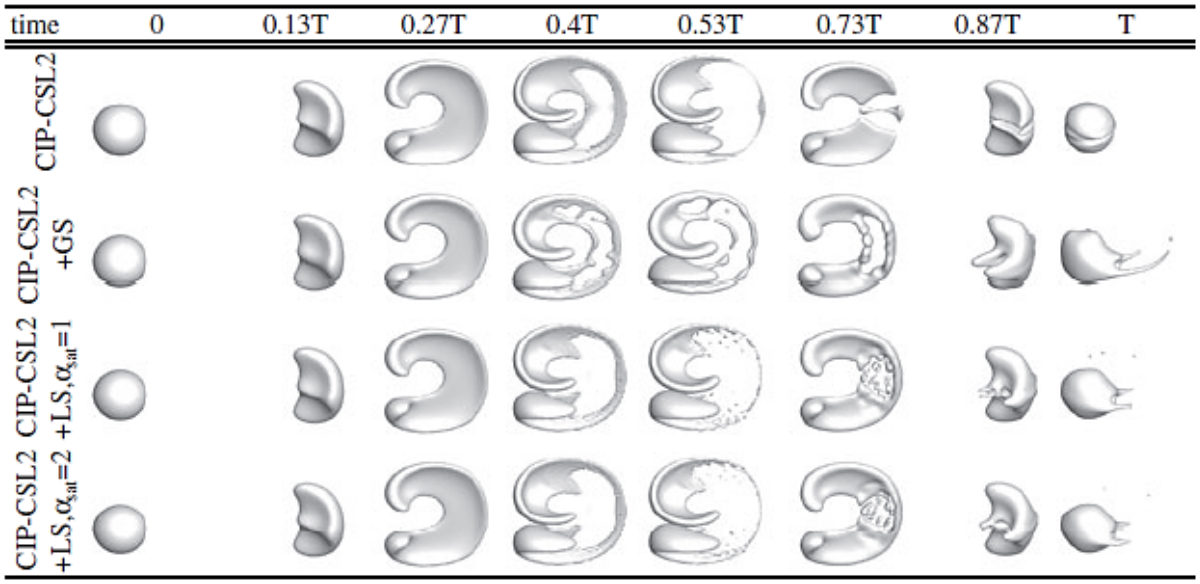

Figure 4. Expected results for CVOFLS validation problem (Sato and Niceno [19]).

In Fig. 5 is shown the results of the algorithm developed in this work, by considering T = 1s.

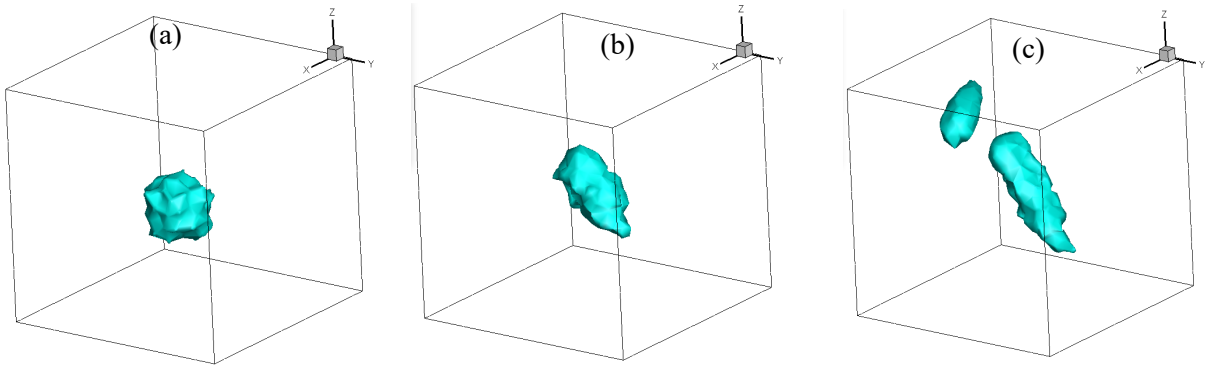

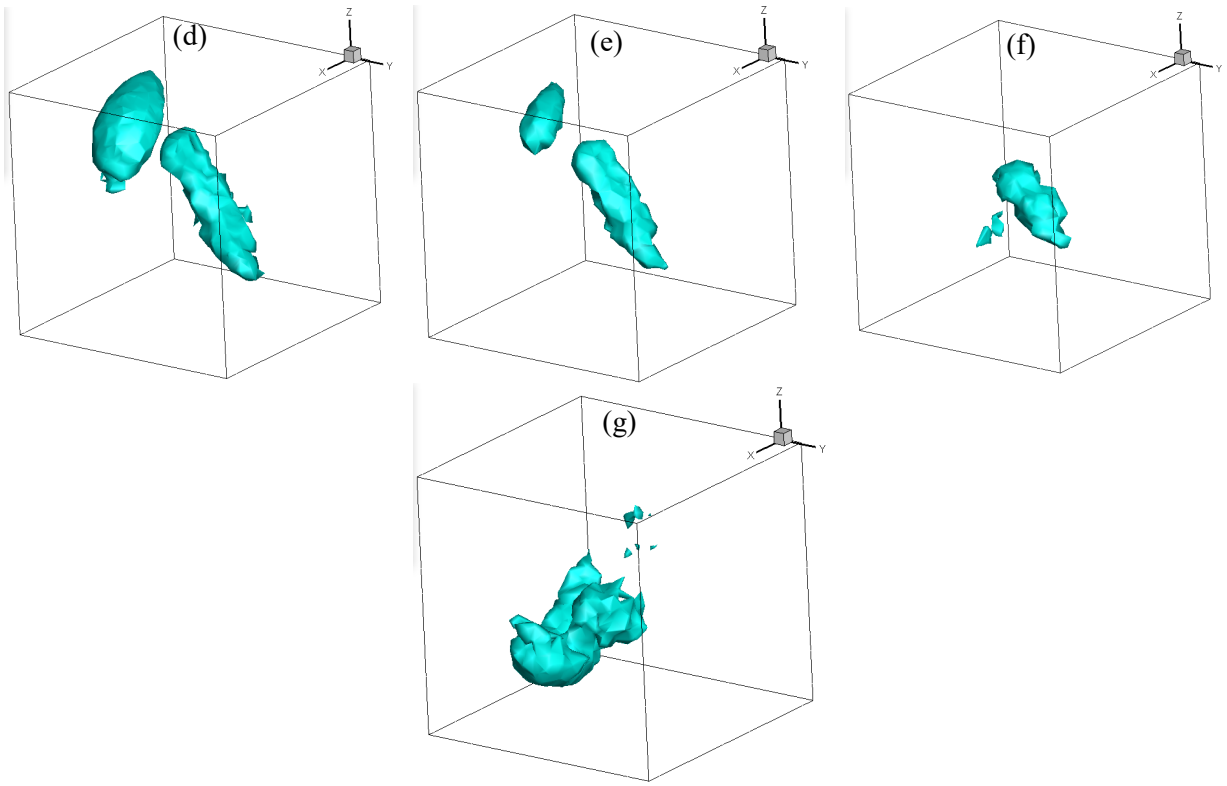

Figure 5. Isovalues of Level Set domain at (a) t=0 and (b) t=0.13T (c) t=0.27T (d) t=0.40T (e) t=0.33T (f) t=0.73T (g) t=T.

One may observe that the implemented code is sensible to the velocity field and it is able to capture the interface over time.

By comparing Fig. 4 and Fig. 5, it is possible to observe that the developed solver still not reproduces the expected results since the vapor bubble shape is not the same. In this way, it is necessary adjusts in the developed code.

5 Preliminary Numerical Results

In order to test the implementation of Equations (12), (13) and (14), an empirical correlation was implemented to bubble growth radius:

$$R\frac{d^2R}{dt^2}+\frac{3}{2}\left(\frac{dR}{dt}\right)^2=-\frac{1}{\rho_f}\left(P_f-P_v+\frac{2\sigma}{R}\right) \tag{20}$$

Figures 6 to 8 show the velocity, pressure, and temperature fields. Figure 9 shows the isovalues of Level Set Function.

At present, the working fluid used was HFE7100 at saturation conditions. It was considered a simulation time of 5 ms, due to the experimental departure time found by the Nest-n group. Moreover, it was assumed a wall superheat degree of 8 °C.

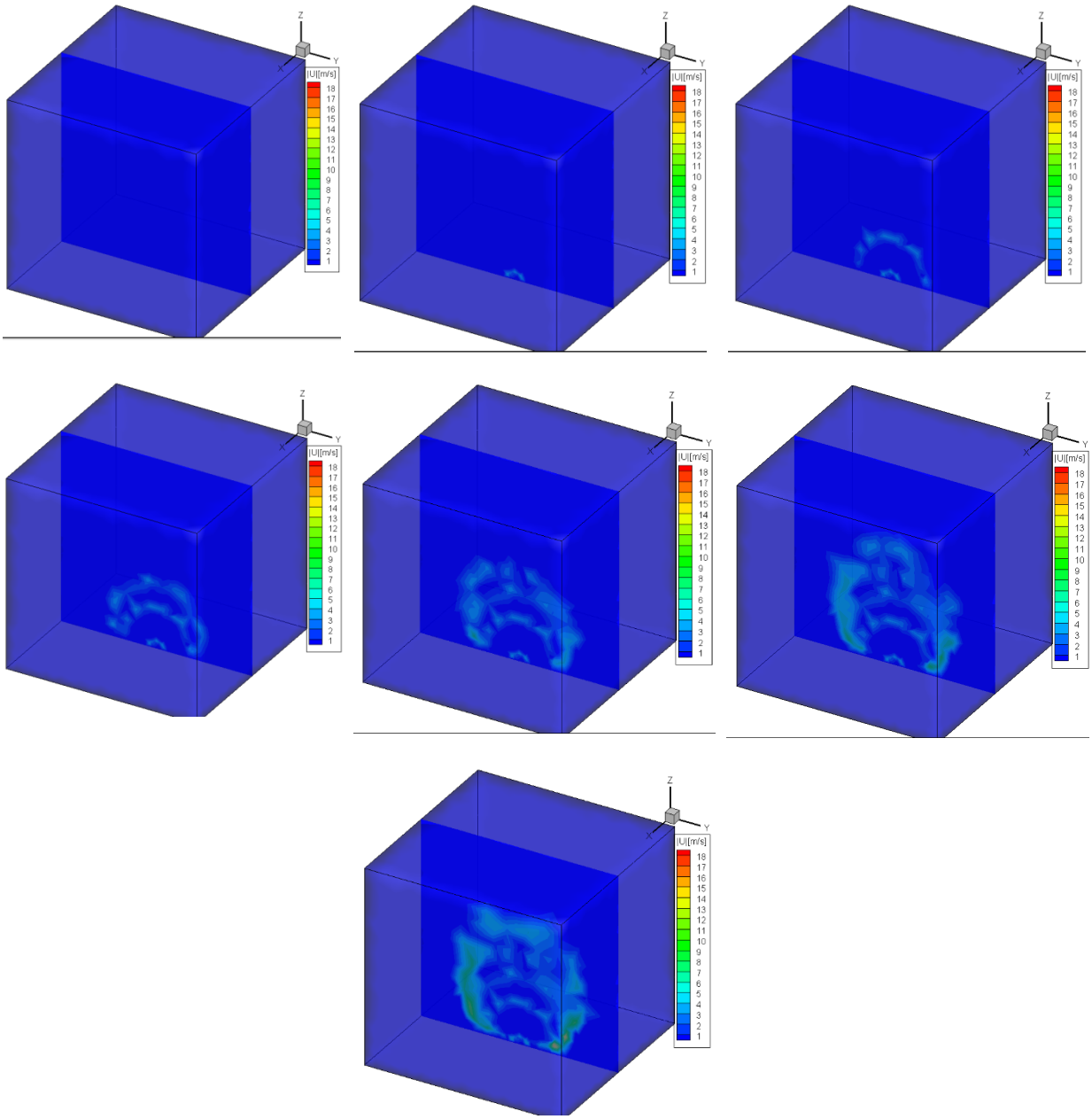

Figure 6. Velocity field in the simulation domain over time with the radius calculated by Eq. (20).

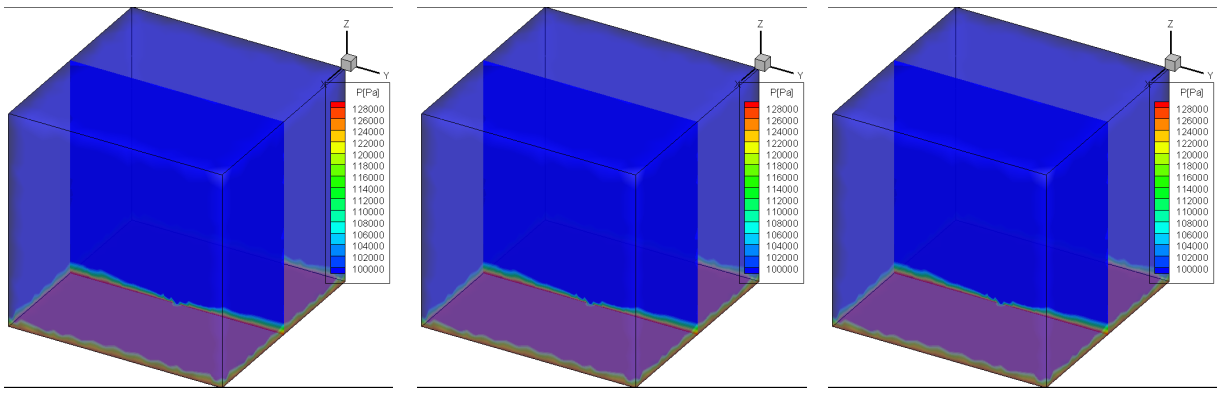

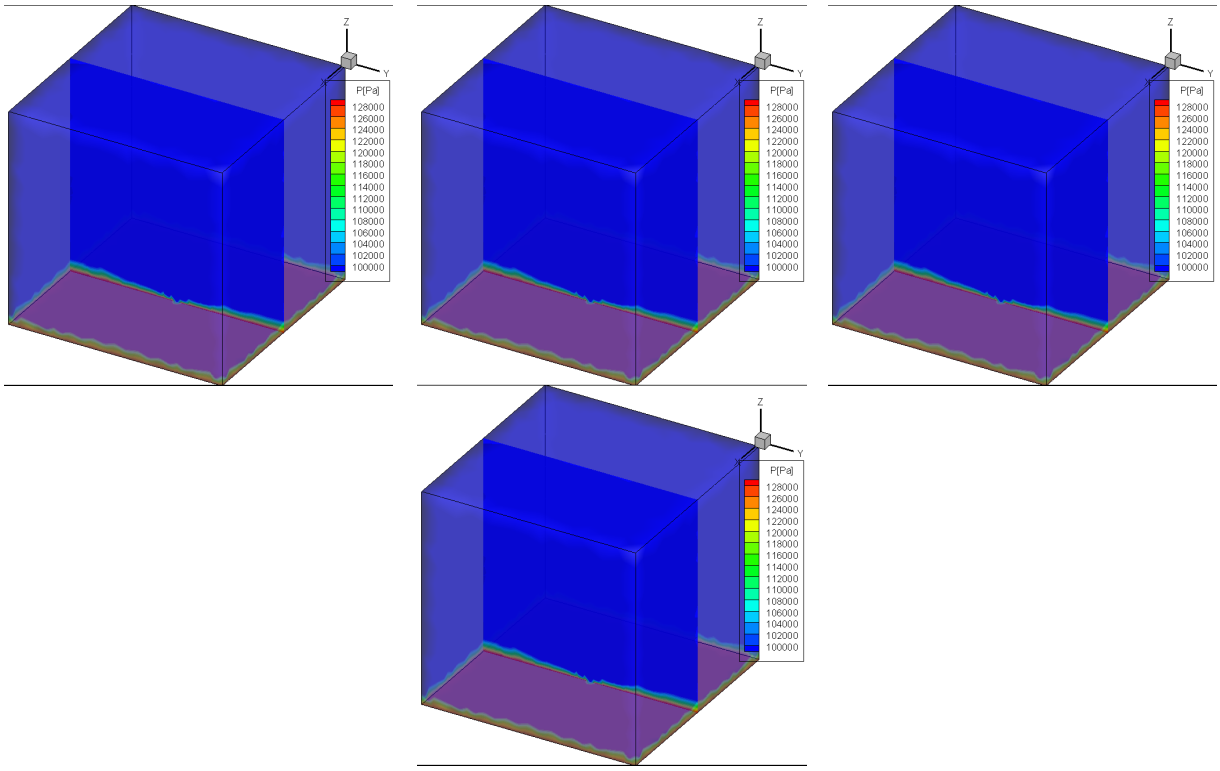

Figure 7. Pressure field in the simulation domain over time with the radius calculated by Eq. (20).

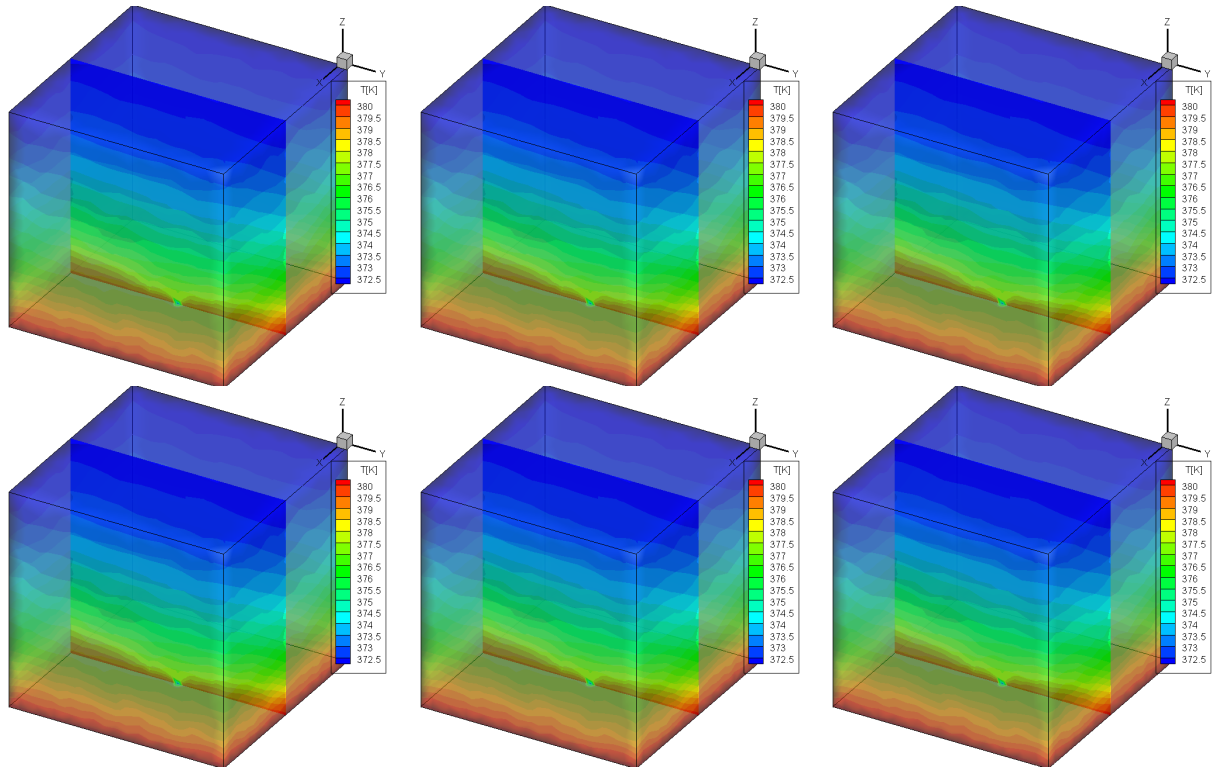

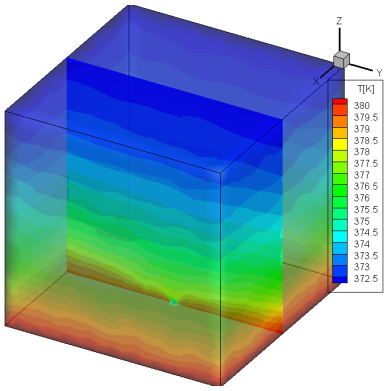

Figure 8. Temperature field in the simulation domain over time with the radius calculated by Eq. (20).

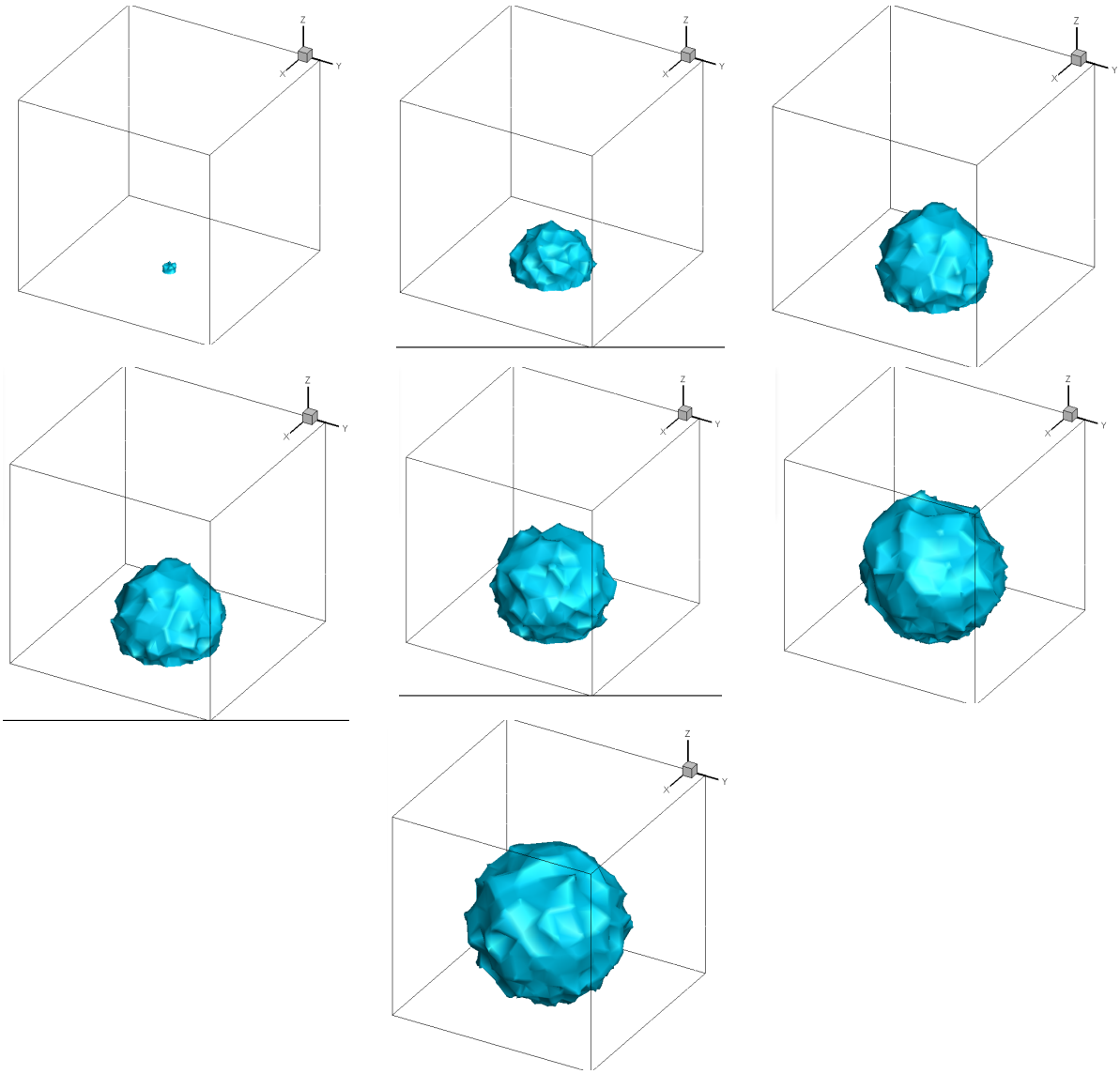

Figure 9. Isovalues of Level Set Function in the simulation domain over time with the radius calculated by Eq. (20).

The developed algorithm well predicts the dynamic contact angle and the bubble shape by using

the Eq. (20). Moreover, the velocity field around the bubble interface is non-zero, showing the interface movement over time (this could be explained by the surface tension and its influence on the momentum equation).

The pressure and temperature fields are coupled with the velocity field and the interfacial forces play an important role in the momentum equation; thus, it is still necessary to revise the advection terms, corresponding to the pressure and energy, in order to analyze the vapor bubble growth over time.

The CLSVOF algorithm was coupled with the boiling problem, without a radius growth, to analyze the numerical behavior. Figures 10 to 13 show the preliminary results.

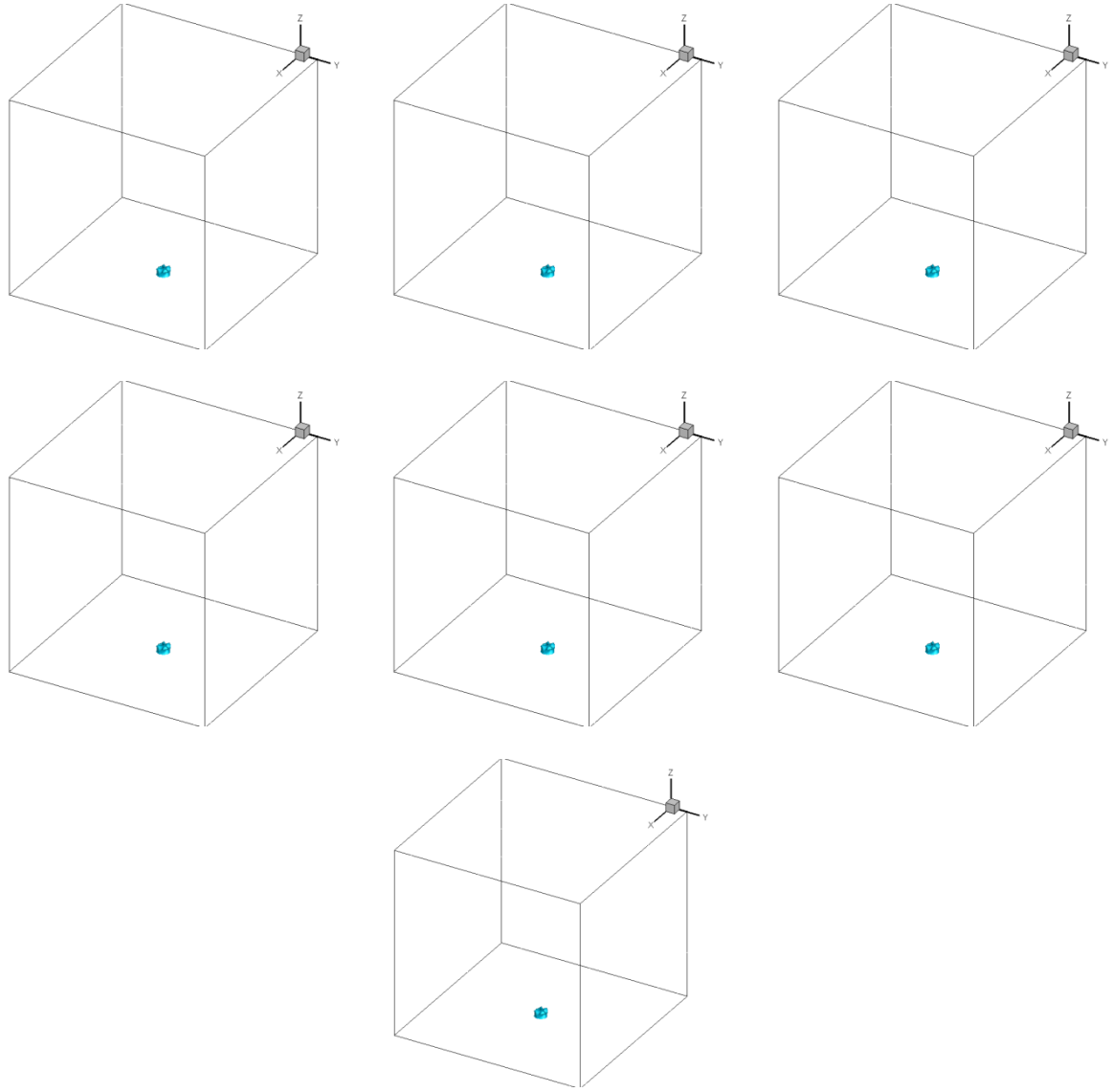

Figure 10. Isovalues of Level Set Function over time coupling the developed CLSVOF method and the governing equations.

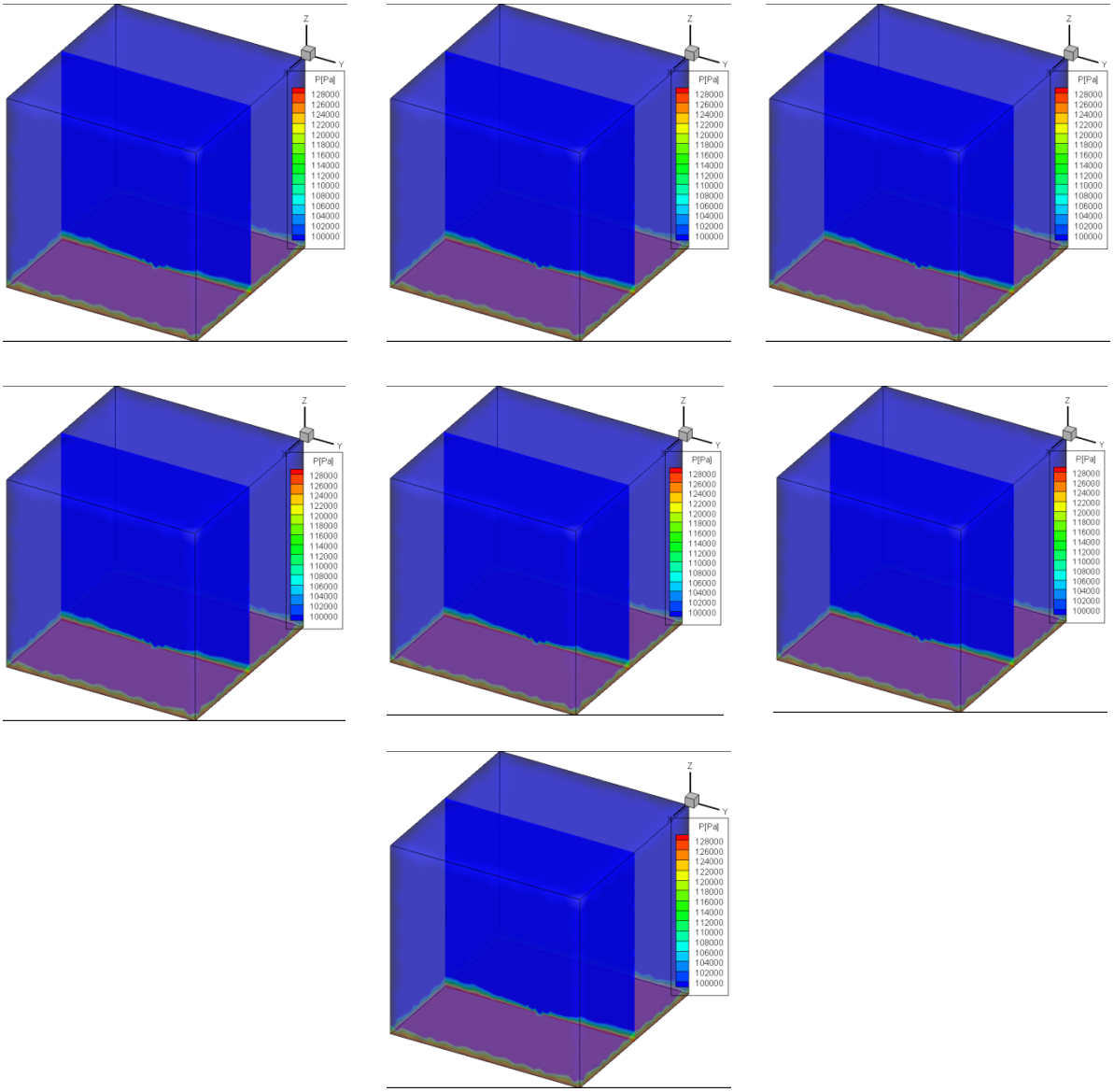

Figure 11. Pressure over time coupling the developed CLSVOF method and the governing equations.

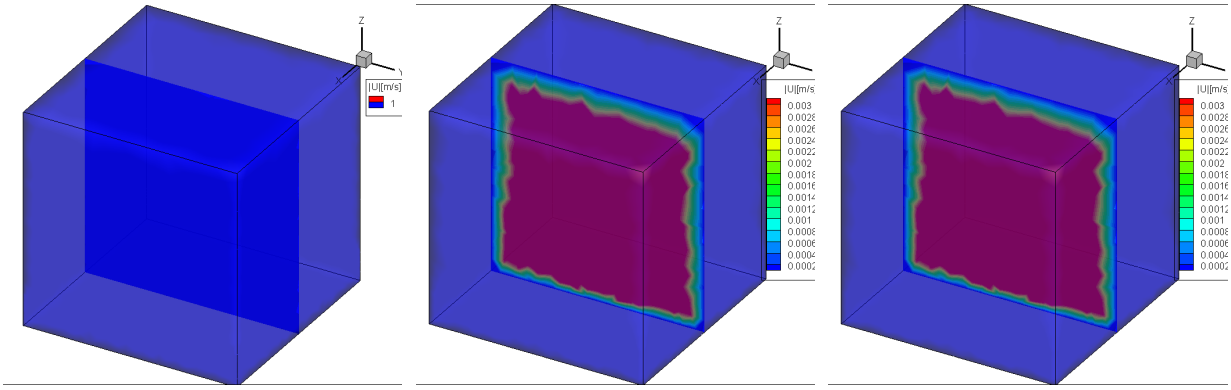

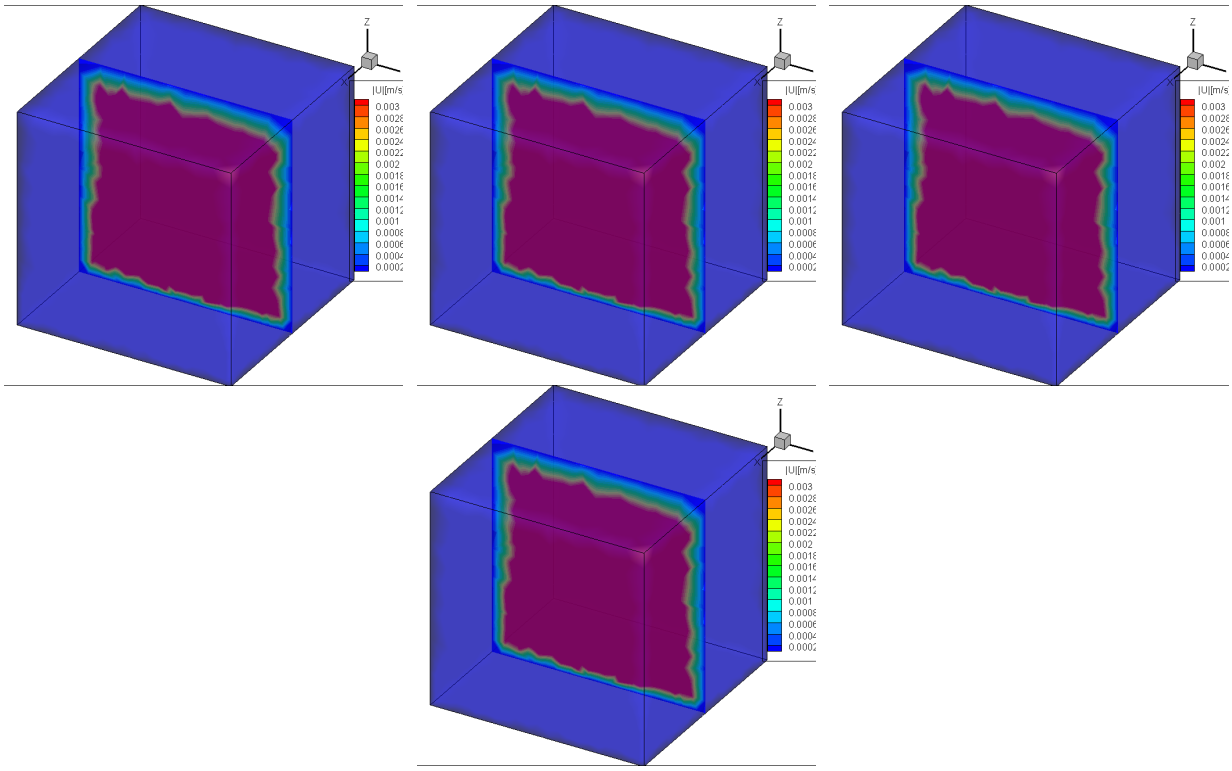

Figure 12. Velocity field over time coupling the developed CLSVOF method and the governing equations.

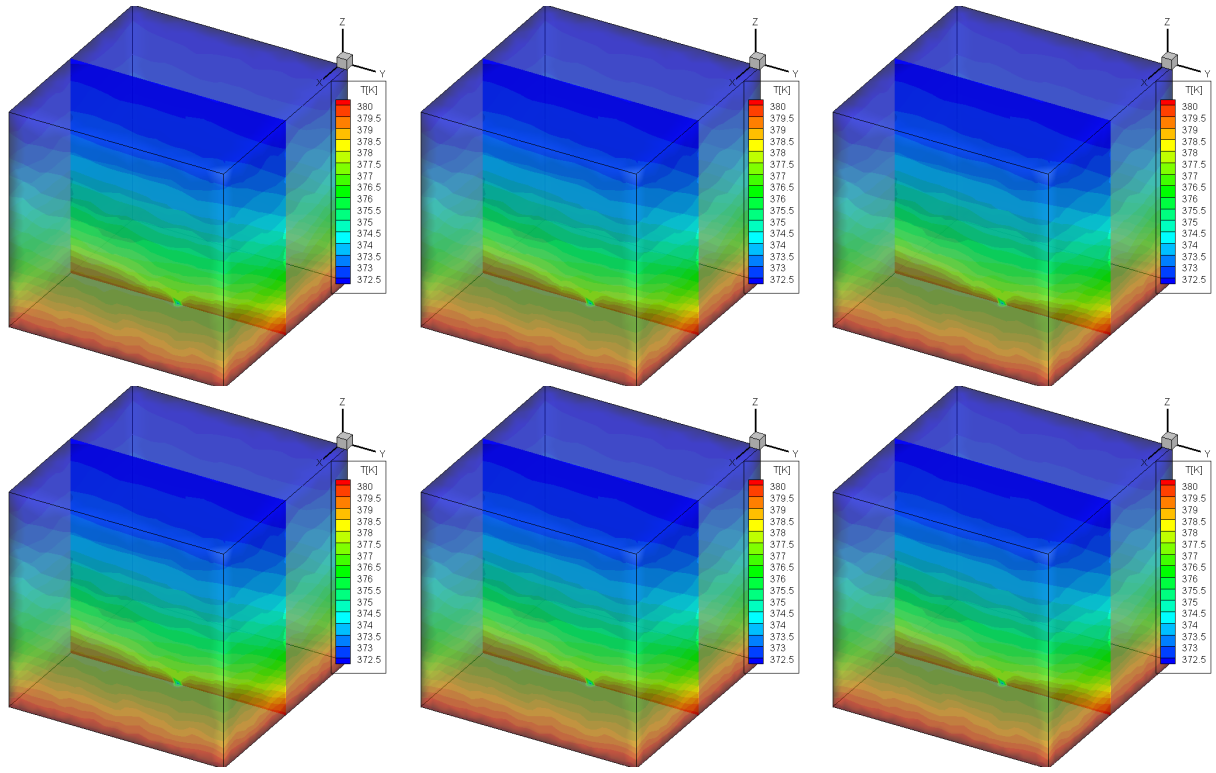

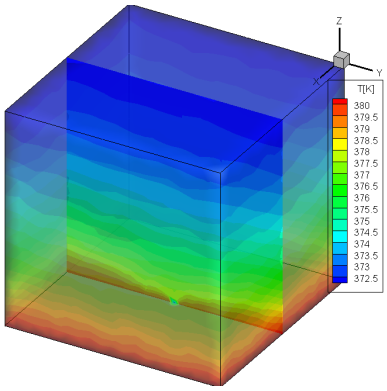

Figure 13. Temperature field over time coupling the developed CLSVOF method and the governing equations.

Figure 12 shows that pool boiling problem, characterized by low heat fluxes, is a diffusive problem, being consistent with the literature. The coupling of CVOFLS with thermo-mechanical equations showed that, for momentum equation, all terms have the same order, leading to a realistic velocity field.

The CVOFLS algorithm is very sensitive to the velocity field; in Fig. 12, the velocity field is almost zero and uniform in all domains, which could explain why Level Set isovalues remains constant over time.

Interfacial velocities were not observed due to the pressure field remains constant over time, showing the need to review the developed code. Moreover, as the temperature field remains constant over time, the algorithm for the energy equation also needs to be reviewed.

6 Comparison between experimental and numerical data

Based on the experimental pool boiling tests performed in the setup described in Fig. 2, it was possible to record the vapor bubble radius over time. Figure 14 presents the evolution in time of the vapor bubble radius obtained by the numerical simulation and the experimental data for the HFE7100 at saturation conditions and for a wall-superheating equal to 14.39 K.

One may observe that Eq. (15) fits well the experimental data, being a good initial guess to capture the vapor bubble interface.

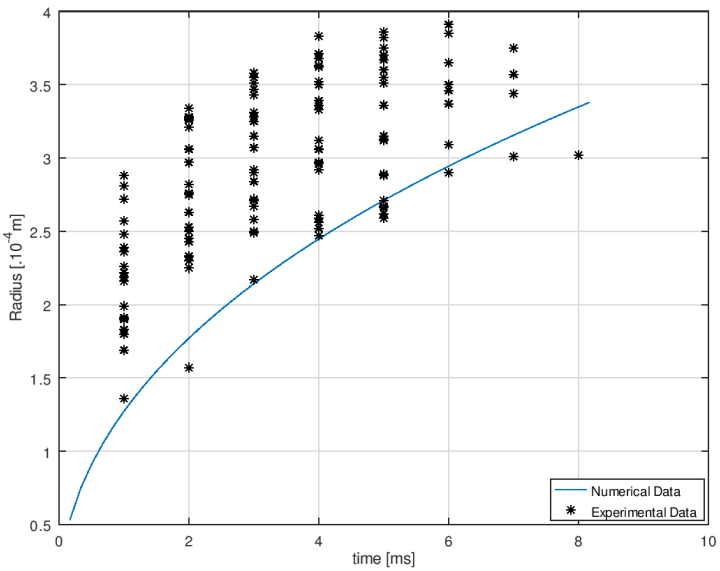

Figure 14. Comparison between numerical and experimental data for the vapor bubble evolution over time.

7 Conclusions

The presented work shows a new methodology of analysis of the pool boiling phenomena. About this methodology can be concluded that:

- The implemented CVOFLS is capable to follow the bubble growth interface and the method is sensitive to the domain's velocity field;
- The theoretical radius used shows good agreement to experimental data and it was able to predict the dynamic contact angle of vapor bubble;
- The thermo-mechanical equations implemented should be revised;
- The implemented Eq. (15) can be used as an initial guess to capture the bubble interface.

Acknowledgments

The authors are grateful for the financial support from FAPESP (grant number 2018/12010-4 and 2019/02566-8) and from UNESP in the performance of this study.

References

[1] Yeom, H.; Sridharan, K.; Corradini, M. L. Bubble Dynamics in Pool Boiling on Nanoparticle-Coated Sur-faces. In: Heat Transfer Engineering, vol. 36, issue 12, pp. 1013-1027. (2015).
[2] Stephan, P., Hammer, J., 1994. A new model for nucleate boiling heat transfer. Warme und Stoffubertra-gung 30, 119–125.
[3] Kawanami, Osamu et al., Experiment on nucleate pool boiling in microgravity by using transparent heating surface – Analysis of surface heat transfer coefficients. Journal of Physics Conference Series. Dec. 2011.
[4] Tai Wang, Hui-Xiong Li, and Jian-Fu Zhao. Three-Dimensional Numerical Simulation of Bubble Dynamics in Microgravity under the Influence of Nonuniform Electric Fields Microgravity Sci. Technol. (2016).
[5] Souza, R.R; Manetti, L.L.; Kiyomura, I.S., Cardoso, E.M. Liquid/surface interaction during pool boiling of DI-water on nanocoated heating surfaces. J. Braz. Soc. Mech. Sci. & Eng., Vol. 40(11) (2018).
[6] R. K. Patil. A numerical model for a bubble in nucleate pool boiling, Ph.D. Thesis, Iowa State University, 1991.
[7] T. M. Shah and N. Talat. A Comparison of Characteristic-Based Split Algorithm and Multi-Grid method for Solution of Incompressible Navier-Stokes Equations. International Journal of Engineering & Technology IJET-IJENS Vol:13 No:05 (2013).
[8] G. A. P. Baggio and J. B. C. Silva. Tridimensional Flow Simulation with Finite Element Stabilized. Proceedings of the XXXVII Iberian Latin-American Congress on Computational Methods in Engineering Suzana Moreira Ávila (Editor), ABMEC, Brasília, DF, Brazil, November 6-9, 2016.
[9] I. Perez-Raya and S. G. Kandlikar. A Volume of Fluid Based Model for the Simulation of Bubble Growth over a Heated Surface. Proceedings of the ASME 2018 16th International Conference on Nanochannels, Microchannels, and Minichannels ICNMM2018 June 10-13, 2018, Dubrovnik, Croatia.
[10] E. Teodori et al. Enhanced VOF-Based Direct Numerical Simulations of Slug Flow Boiling within Micro-Channels with Smooth and Finned Heated Walls. Proceedings of the 16th International Heat Transfer Conference, IHTC-16 August 10-15, 2018, Beijing, China.
[11] Albadawi, A., Donoghue, D.B., Robinson, A.J., Murray, D.B., Delauré, Y.M.C., On the assessment of a VOF based compressive interface capturing scheme for the analysis of bubble impact on and bounce from a flat horizontal surface, International Journal of Multiphase Flow (2014), DOI: http://dx.doi.org/10.1016/j.ijmultiphaseflow.2014.05.017.
[12] F. Giboua, R. Fedkiwc, and S. Osherd. A review of level-set methods and some recent applications. Journal of Computational Physics 353 (2018) 82–109.

[13] S. Menon. A course at Chalmers University of Technology: Coupled Level-Set with VOF interFoam. (2016).
[14] K. Ling, Z.H. Li a, D.L. Sun, Y.L. He, W.Q. Tao. A three-dimensional volume of fluid & level set (VOSET) method for incompressible two-phase flow. Computers & Fluids 118 (2015) 293–304.
[15] A. Albadawi, D.B. Donoghue, A.J. Robinson, Murray, Y.M.C. Delauré. Influence of surface tension implementation in Volume of Fluid and coupled Volume of Fluid with Level Set methods for bubble growth and detachment. International Journal of Multiphase Flow 53 (2013) 11–28.
[16] Pastuszko, Robert. Pool boiling for extended surfaces with narrow tunnels – Visualization and a simplified model. Experimental Thermal and Fluid Science 38 (2012) 149–164.
[17] Y. Sato, B. Niceno. Nucleate pool boiling simulations using the interface tracking method: Boiling regime from discrete bubble to vapor mushroom region. International Journal of Heat and Mass Transfer 105 (2017) 505–524.
[18] William H. Press et al. Numerical Recipes in Fortran 77. London: Cambridge University Press, 1996.
[19] Y. Sato and B. Niceno. A conservative local interface sharpening scheme for the constrained interpolation profile method. INTERNATIONAL JOURNAL FOR NUMERICAL METHODS IN FLUIDS 2012; 70:441–467 Published online 17 October 2011 in Wiley Online Library (wileyonlinelibrary.com/journal/nmf). DOI: 10.1002/fld.2695.